Integrative Biology

Dynamic Article Links

Cite this: *Integr. Biol.*, 2012, **4**, 672–684

www.rsc.org/ibiology

PAPER

Monitoring of the prostate tumour cells redox state and real-time proliferation by novel biophysical techniques and fluorescent staining

Michal Masarik,*[a] Jaromir Gumulec,[a] Marian Hlavna,[ac] Marketa Sztalmachova,[ab] Petr Babula,[c] Martina Raudenska,[a] Monika Pavkova-Goldbergova,[a] Natalia Cernei,[bd] Jiri Sochor,[bd] Ondrej Zitka,[bd] Branislav Ruttkay-Nedecky,[b] Sona Krizkova,[b] Vojtech Adam[bd] and Rene Kizek[bd]

Received 5th November 2011, Accepted 6th April 2012
DOI: 10.1039/c2ib00157h

The present paper is focused on zinc(II) treatment effects on prostatic cell lines PC-3 (tumour) and PNT1A (non-tumour). Oxidative status of cells was monitored by evaluation of expression of metallothionein (MT) isoforms 1A and 2A at the mRNA and protein level, glutathione (oxidised and reduced), and intracellular zinc(II) after exposition to zinc(II) treatment at concentrations of 0–150 μM using electrochemical methods, western blotting and fluorescent microscopy. A novel real-time impedance-based growth monitoring system was compared with widely used end-point MTT assay. Impedance-based IC_{50} for zinc(II) is 55.5 and 150.8 μM for PC-3 and PNT1A, respectively. MTT-determined IC_{50} are >1.3-fold higher. Impedance-based viability correlates with viable count ($r > 0.92$; $p < 0.03$), not with MTT. Two-fold lower intracellular zinc(II) in the tumour PC-3 cell line was found. After zinc(II) treatment >2.6-fold increase of intracellular zinc(II) was observed in non-tumour PNT1A and in tumour PC-3 cells. In PC-3 cells, free and bound zinc(II) levels were enhanced more markedly as compared to PNT1A. PNT1A produced 4.2-fold less MT compared to PC3. PNT1A cells showed a 4.8-fold increase trend ($r = 0.94$; $p = 0.005$); PC-3 did show a significant trend at MT1 and MT2 protein levels ($r = 0.93$; $p = 0.02$) with nearly ten-fold increase after 100 μM zinc(II) treatment. In terms of redox state, PNT1A had a predominance of reduced GSH forms (GSH : GSSG ratio > 1), when exposed to zinc(II) compared to PC3, where predominance of oxidised forms remains at all concentrations. IC_{50} differs significantly when determined by MTT and real-time impedance-based assays due to dependence of impedance on cell morphology and adhesion. When real-time growth monitoring, precise electrochemical methods and fluorescent microscopy are performed together, accurate information for metal fluxes, their buffering by thiol compounds and monitoring of the redox state become a powerful tool for understanding the role of oxidative stress in carcinogenesis.

[a] *Department of Pathological Physiology, Faculty of Medicine, Masaryk University, Kamenice 5, CZ-625 00 Brno, Czech Republic. E-mail: masarik@med.muni.cz; Fax: +420-5-4949-4340; Tel: +420-5-4949-3631*
[b] *Department of Chemistry and Biochemistry, Faculty of Agronomy, Mendel University in Brno, Zemedelska 1, CZ-613 00 Brno, Czech Republic*
[c] *Department of Natural Drugs, Faculty of Pharmacy, University of Veterinary and Pharmaceutical Sciences, Palackeho 1-3, CZ-612 42 Brno, Czech Republic*
[d] *Central European Institute of Technology, Brno University of Technology, Technicka 3058/10, CZ-616 00 Brno, Czech Republic*

Insight, innovation, integration

Prostate cancer cells have altered the ability to uptake and accumulate zinc(II) ions compared to healthy prostate tissue, however, the mechanism is not clear, but it is obvious that some thiols such as metallothionein and glutathione can be involved. This study was focused on zinc(II) treatment effects on the PC-3 prostate cancer cell line and the PNT1A cell line representing non-tumorous prostate epithelial cells. We suggested, optimized and applied various methods and protocols to monitor redox status, gene expression of metallothionein isoforms 1A and 2A at the RNA and protein level, reduced and oxidized glutathione content. In addition, this study describes application of a new label-free and non-invasive method based on impedance determination for real-time analysis of cell proliferation, adhesion and spreading.

Introduction

It has been repeatedly reported that prostate cancer cells are characterised by altered ability to uptake and accumulate zinc(II) ions as compared to healthy prostate tissue.[1] In fact, there is no evidence or records on prostate tumours with unchanged ability to accumulate zinc. In healthy tissue, zinc(II) plays an important role in proliferation, differentiation regulation and apoptosis in prostate (Fig. 1).[2] In healthy and tumour prostate, intracellular zinc(II) is buffered by numerous proteins (metalloenzymes, nucleoproteins and metalloproteins, in particular metallothioneins).[3] Metallothioneins (MTs) are ubiquitous low-molecular mass cysteine-rich proteins, playing a key role in maintaining zinc(II) homeostasis. They are also involved in the protection of cells against oxidative stress in association with reduced glutathione (GSH).[4] Due to these functions, it is natural that MTs are overexpressed under conditions with the increased risk of reactive oxygen species formation, such as cell proliferation, embryonic development or carcinogenesis.[4b,5] Due to MTs' low molecular mass and unique primary structure, commonly used methods for detection of proteins suffer from many deficiencies including insufficient specificity and sensitivity. The most frequent methods used for the detection of these proteins are immunological and/or electrochemical ones with the lowest detection limits at aM concentrations.[6]

This study was focused on zinc(II) treatment effects on the PC-3 prostate cancer cell line and the PNT1A cell line representing non-tumorous prostate epithelial cells. Particularly, monitoring of redox status influenced by zinc(II) ions was performed, in particular gene expression of metallothionein isoforms 1A and 2A at the RNA and protein level. In addition to redox status, reduced and oxidized glutathione was also determined. Moreover, cell viability and proliferation after zinc(II) ions treatment were studied since cell viability, adhesion and spreading can be affected by the cell redox state.[7] In addition, this study describes application of a new label-free and non-invasive method based on impedance determination for real-time analysis of cell proliferation, adhesion and spreading. Together with utilization of electrochemical methods for determination of some biochemical markers, such comprehensive results have not been obtained yet on tumour and non-tumour prostate cell lines.

Experimental

Chemical and biochemical reagents

Commercial materials were obtained as follows: RPMI-1640 medium, Ham's F12 medium, foetal bovine serum (FBS) – mycoplasma free, penicillin/streptomycin and trypsin EDTA were purchased from PAA Laboratories GmbH (Austria). PBS was purchased from Invitrogen Corp. (USA). EDTA, zinc(II) sulphate, RIPA buffer and all other chemicals of ACS purity were purchased from Sigma Aldrich Co. (USA), unless noted otherwise. Primary mouse metallothionein antibody and secondary anti-mouse HRP conjugated antibody were purchased from Abcam (USA), primary PSA antibody was purchased from Santa Cruz Biotechnology Inc (USA). For chemiluminescent detection of western blot membranes an ECL WB detection reagents system from Amersham Pharm. biotech was used (USA).

Cell cultures

Two human prostatic cell lines were used in this study: (a) PNT1A human cell line established by immortalisation of normal adult prostatic epithelial cells by transfection with a plasmid containing SV40 genome with a defective replication origin. The primary culture was obtained from the normal prostatic tissue of a 35 years old male at post-mortem; (b) PC-3 human cell line established from a grade 4 prostatic adenocarcinoma from

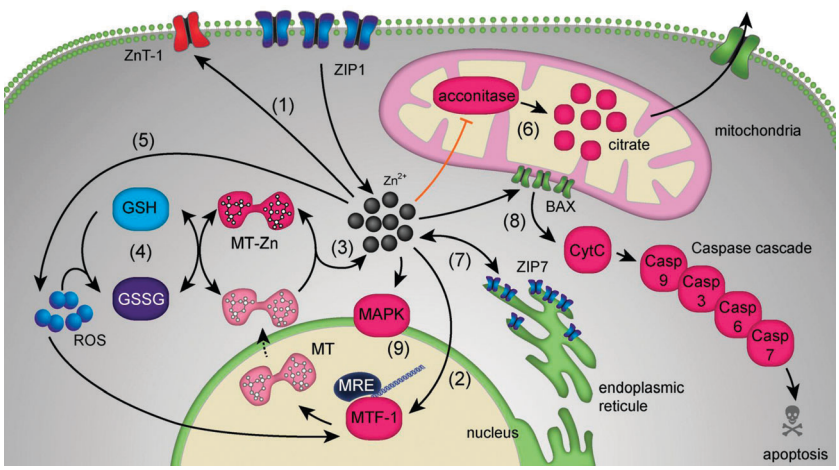

Fig. 1 Effect of zinc(II) in prostatic tissue. ZIP and ZnT maintain intracellular zinc transport (1); ZIP1 is a major zinc(II) importer, ZnT-1 is the only export transporter. Intracellular free zinc(II) induces metallothionein (MT) expression through MTF-1 and MRE (2) and is buffered by MT (3) (white MT represents reduced/metal-free form, grey MT represents oxidized/metal-bound form). High zinc(II) load induces oxidative stress (ROS) (5), which is reduced by the glutathione system in cooperation with MT (4); MT converts glutathione to its reduced form while being oxidized. Endoplasmic reticulum regulates the cytoplasmic free zinc level by ZIP7 transporter (7). Free zinc(II) affects gene expression through a mitogen-activated protein kinase cascade (MAPKs, 9). In prostate, a high zinc(II) level inhibits mitochondrial aconitase (mAC), thus citrate is accumulated (6) and released in high levels. Zinc induces a prostate-specific BAX pore formation (8) causing cytochrome C (CytC) release from mitochondria and subsequent caspase-mediated apoptosis. Adapted according to Franklin and Costello[30] and Eckschlager *et al.*[4b]

a 62 years old Caucasian male and derived from the metastatic site in bone. Both cell lines used in this study were purchased from HPA Culture Collections (Salisbury, UK).

Cultured cell conditions

PNT1A cells were cultured in RPMI-1640 medium with 10% FBS. PC-3 were cultured in Ham's F12 medium with 7% FBS. All media were supplemented with penicillin (100 U ml^{-1}) and streptomycin (0.1 mg ml^{-1}), and the cells were maintained at 37 °C in a humidified incubator with 5% CO_2. The passages of PNT1A and PC-3 cell lines ranged from 10 to 35.

Zinc(II) treatments of cell culture

Once the cells grew up to 50–60% confluence of the culture, the growth media were replaced by fresh medium for 24 h to synchronize cell growth. The cells were then treated with or without zinc(II) sulphate (0–100 μM for both cell lines) in fresh medium for 48 h. In the case of viability and proliferative assays (MTT and xCELLigence measurements) cells were treated with a concentration of 300 μM.

Sample preparation

RIPA buffer lysate. Cell line's medium was removed and samples were quickly rinsed with 5 ml of ice-cold PBS twice. Cells were scraped, transferred to clean tubes and were centrifuged at 800 × *g* for 5 minutes (Eppendorf 5402, Germany) at room temperature. Then the cell pellet was transferred to 1.5 ml tubes and washed with PBS twice and centrifuged at 800 × *g* for 5 minutes again. RIPA buffer was added and tubes were intermittently mixed for 15 minutes on ice by vortexing. Then, samples were centrifuged at 20 800 × *g* for 15 min at 4 °C and the supernatant was used for further analysis.

Thermo-lysate. Approximately 0.01 g of the cells in 500 μl of PBS was mechanically disintegrated using an Ultra-Turrax T8 homogenizer (Ika, Germany) placed in an ice bath for 3 min at 25 000 rpm. The cell homogenates were kept at 99 °C in a thermomixer (Eppendorf 5430, Germany) for 15 min with shaking. The denatured homogenates were centrifuged at 4 °C, 15 000 × *g* for 30 min (Eppendorf 5402, Germany). Heat treatment effectively denatures and removes thermolabile and high molecular mass proteins out from the samples.[8] The prepared samples were used for metallothionein and GSH/GSSG analyses.

RNA isolation, cDNA preparation

For RNA isolation a High pure total RNA isolation kit (Roche, Switzerland) was used. Cell line's medium was removed and samples were quickly rinsed with 5 ml of ice-cold PBS twice. Cells were scraped, transferred to clean tubes and centrifuged at 20 800 × *g* for 5 min at 4 °C. After this step, lysis buffer was added and RNA isolation was carried out according to manufacturer's instructions. Isolated RNA was used for cDNA synthesis. 600 ng of total RNA was transcribed using a Transcriptor first strand cDNA synthesis kit (Roche, Switzerland) according to manufacturer's instructions. 20 μl of prepared cDNA was diluted with RNase free water to 100 μl and directly analysed by real-time PCR.

Real-time reverse-transcription polymerase chain reaction (RT-PCR)

RT-PCR was performed in triplicate using the TaqMan gene expression assay system with the 7500 real-time PCR system (Applied Biosystems, USA). The amplified DNA was analysed by the comparative Ct method using β-actin as an endogenous control. The primer and probe sets for β-actin (Assay ID: Hs00185826_m1), MT1 Assay ID: Hs00185826_m1) and MT2 (Hs00794796_m1) were selected from TaqMan gene expression assay. Real-time PCR was performed under the following amplification conditions: total volume of 20 μl, initial denaturation 95 °C per 10 min, than 45 cycles 95 °C per 15 s, 60 °C per 1 min.

Cell content quantification

Total cell content was analysed using a Cedex XS (Innovatis) semi-automated image-based cell analyser according to manufacturer's instructions. Cell line's medium was removed and samples were washed with 5 ml of ice-cold PBS twice to maintain only viable cells. Cells were scraped and transferred to clean tubes. Trypan blue solution (Innovatis) was diluted to 0.2% before use and was added to samples according to manufacturer's manual. Following settings were used in operating software: cell type: standard cells, dilution: none, process type: standard. All samples were measured in duplicates.

Measurements of cell viability – MTT test

The MTT assay was used to determine cell viability. The suspension of cells in growth medium was diluted to a density of 5×10^3 cells per ml and 200 μl were transferred to 2–11 wells of standard microtiter plates. Medium (200 μl) was added to the first and to the last column (1 and 12). Plates were incubated for 2 days at 37 °C to ensure cell growth. Medium was removed from columns 2 to 11. Columns 3 to 10 were filled with 200 μl of medium containing different concentrations of zinc (0, 25, 50, 75 and 100 μM). As control, columns 2 and 11 were fed with medium without drug. Plates were incubated for 24 hours; then, all media were removed and exchanged with a fresh medium, daily three times. After that, columns 1 to 11 were fed with 200 μl of medium with 50 μl of MTT (5 mg ml^{-1} in PBS) and incubated for 4 h in a humidified atmosphere at 37 °C, wrapped in aluminium foil. After that, medium-MTT was exchanged with 200 μl of 99.9% DMSO to dissolve MTT-formazan crystals. Then, 25 μl of glycine buffer was added to all wells with DMSO and the absorbance was recorded at 570 nm (VersaMax microplate reader, Molecular devices).

Cell growth and proliferation assay using impedance measurement with the xCELLigence system

The xCELLigence system was used according to the instructions of the supplier (Roche Applied Science and ACEA Biosciences). The xCELLigence system consists of four main components: the RTCA analyser, the RTCA DP station, the RTCA computer with integrated software and disposable E-plate 16. Firstly, the optimal seeding concentration for proliferation and cytotoxic assay was determined. After seeding the total number of cells in 200 μl medium to each well in E-plate 16, the attachment, proliferation and spreading of the cells were monitored every 15 min. All experiments were carried out for 200 h.

Total proteins quantification – Bradford and Biuret methods

Protein amount in cell lysates was measured spectrometrically by the Bradford method and verified by the Biuret method on an automated analyser. The Bradford method was performed on an MBA 2000 analyser (Perkin Elmer, USA) at a wavelength of 595 nm. Total protein amount was determined using the automated biochemical analyzer BS-200 (Mindray, China). Reagents and samples handling were controlled by BS-200 software (Mindray). The absorbance was measured at 510 nm.

Differential pulse voltammetry – Brdicka reaction

Differential pulse voltammetric measurements were performed with a 747 VA Stand instrument connected to a 746 VA Trace Analyzer and a 695 Autosampler (Metrohm, Switzerland), using a standard cell with three electrodes and a cooled sample holder (4 °C). A hanging mercury drop electrode (HMDE) with a drop area of 0.4 mm^2 was the working electrode. An Ag/AgCl/3 M KCl electrode was the reference and a glassy carbon electrode was auxiliary. For data processing GPES 4.9 supplied by EcoChemie was employed. The analysed samples were deoxygenated prior to measurements by purging with argon (99.999%) and saturated with water for 120 s. The Brdicka supporting electrolyte containing 1 mM $Co(NH_3)_6Cl_3$ and 1 M ammonia buffer (NH_3(aq.) + NH_4Cl, pH = 9.6) was used. The supporting electrolyte was exchanged after each analysis. The parameters of the measurement were as follows: an initial potential of −0.7 V, an end potential of −1.75 V, a modulation time of 0.057 s, a time interval of 0.2 s, a step potential of 2 mV, a modulation amplitude of −250 mV, E_{ads} = 0 V, volume of the injected sample: 20 μl (100 × diluted sample with 0.1 M phosphate buffer, pH 7.0). All experiments were carried out at a temperature of 4 °C employing thermostat Julabo F25 (Labortechnik GmbH, Germany).

Electrochemical determination of zinc(II) ions

An electrochemical analyser (Metrohm AG, Switzerland) was used for determination of Zn(II). The analyser (757 VA Computrace from Metrohm, Herisau, Switzerland) employs a conventional three-electrode configuration with a hanging mercury drop electrode (HMDE) as the working electrode: 0.4 mm^2, Ag/AgCl/3M KCl as the reference electrode, and a platinum auxiliary electrode. The following setup assembled for automated voltammetric analysis is supplied by Metrohm. A sample changer (Metrohm 813 Compact Autosampler) performs the sequential analysis of up to 18 samples in plastic test tubes. For the addition of standard solutions and reagents, two automatic dispensers (Metrohm 765 Dosimat) are used, while two peristaltic pumps (Metrohm 772 Pump Unit, controlled by an Metrohm 731 Relay Box) are employed for transferring the rinsing solution into the voltammetric cell and for removing solutions from it. Differential pulse voltammetric measurements were carried out under the following conditions: deoxygenating with argon for 60 s; deposition potential: −1.3 V; time of deposition: 240 s; start potential: −1.3 V; end potential: 0.15 V; pulse amplitude: 0.025 V; pulse time: 0.04 s; step potential: 5.035 mV; time of step potential: 0.3 s.

Determination of low-molecular-mass thiols

A high performance liquid chromatograph with an electrochemical detection (HPLC-ED) system consisted of two solvent delivery pumps operating in the range of 0.001–9.999 ml min^{-1} (Model 582 ESA Inc., Chelmsford, MA), a Zorbax Eclipse AAA Column (4.6 × 150 mm 3.5 micron particle size; Varian Inc., CA, USA), and a CoulArray electrochemical detector (Model 5600A, ESA, USA). The sample (30 μl) was injected using an autosampler (Model 540 Microtiter HPLC, ESA, USA). HPLC-ED experimental conditions were as follows – mobile phase compositions: A: 80 mM trifluoroacetic acid and B: methanol. They were mixed in gradient from 3% B in the 1st min, 10% B in the 2nd to the 6th min and 98% B from the 7th min of separation; flow of the mobile phase was 0.8 ml min^{-1}, temperature of the separation was 40 °C; working electrodes potential was 900 mV; detector temperature was 30 °C; each measurement was repeated three-times. Retention time of the reduced glutathione (GSH) was 5 min. GSH concentration was calculated from a calibration curve (0.5–100 μM). The signal was quantified as a sum of current responses from all working electrodes.[9] In the case of real sample measurements, the shift of the retention time was about ±2%.

Western blotting analysis

Samples were prepared (4 μl of DTT and 8 μl of LDS buffer, 4 μl of sample per well) and incubated for 5 minutes at 37 °C. Electrophoresis was done on 10% and 12% 0.75 mm SDS-PAGE gels at 100 V for 90 minutes. After the electrophoretic separation, the proteins were transferred onto a nitrocellulose membrane (Bio-Rad, USA) in a Bio-rad apparatus (Bio-Rad, USA). The blotting was carried out for 1 h at a constant current of 0.9 mA for 1 cm^2 of the membrane. After the transfer, the membrane was blocked with 5% non-fat milk in PBS (137 mM NaCl, 2.7 mM KCl, 1.4 mM NaH_2PO_4, and 4.3 mM Na_2HPO_4; pH 7.4) for 2 hours. The incubation with the mouse primary antibody in dilution of 1 : 750 in PBS with 5% non-fat milk was carried out for 12 h at 4 °C. After washing three times with PBS containing 0.05% (v/v) Tween-20 (PBS-T) for 5 min the membrane was incubated with a secondary antibody (anti-mouse labelled with horseradish peroxidase, Sigma Aldrich Co., diluted 1 : 5000) for 1 h at room temperature. Then, the membrane was washed three times with PBS-T for 5 min and incubated with a chromogenic substrate (0.4 mg ml^{-1} AEC – 3-aminoethyl-9-carbazole in 0.5 M acetate buffer with 0.1% H_2O_2, pH 5.5).

Fluorescence microscopy and cell staining

For fluorescence microscopy, cells were cultivated directly on microscope glass slides (75 × 25 mm, thickness 1 mm, Fischer Scientific, Czech Republic) in Petri dishes in the above-described cultivation media (see Cultured cell conditions). Cells were transferred directly onto slides, which were submerged in cultivation media. After treatment, microscope glass slides with a monolayer of cells were removed from Petri dishes, rinsed with cultivation medium without zinc(II) supplementation and PBS buffer and directly used for staining and fluorescence microscopy.

For the staining of free thiols, respectively, free –SH groups, 5-(bromomethyl)fluorescein (5-BMF, Sigma-Aldrich, USA) was used. This probe reacts more slowly with thiols of peptides, proteins and thiolated nucleic acids in comparison with other fluorescent probes. However, it forms stronger thioether bonds that are expected to remain stable under the conditions required for fluorescence microscopy. Stock solution of 5-BMF (4 mM, anhydrous dimethyl sulfoxide) was prepared prior to staining because of 5-BMF stability. Working solution was prepared immediately using stock solution by diluting to a final concentration of 20 μM (PBS buffer, pH = 7.6). Cells were incubated for one hour at 37 °C and in the dark. Then, cells on the microscope glass slide were washed with PBS buffer (pH = 7.6) and observed using a fluorescence microscope (Axioskop 40, Carl Zeiss, Germany) equipped with wideband excitation and set of filters (FITC-DAPI, Carl Zeiss, Germany). Photographs were taken using a digital camera (Olympus Camedia 750, Olympus, Japan).

For free zinc(II) ions staining, fluorescent probe *N*-(6-methoxy-8-quinolyl)-*p*-toluene sulphonamide (TSQ, Invitrogen, USA) was used. Working solution (10 μM, phosphate buffer, pH = 7.6) was prepared by diluting TSQ stock solution (10 mM, acetone). Cells were carefully rinsed by PBS buffer to remove all cultivation media containing free zinc(II) ions, subsequently stained by working TSQ solution (30 min, 37 °C, dark), washed with PBS buffer (pH = 7.6) and observed under a fluorescence microscope (Axioskop 40, Carl Zeiss, Germany) equipped with FITC and DAPI filters (Carl Zeiss, Germany). Photographs were taken on a digital camera (Olympus Camedia 750, Olympus, Japan).

Statistical data analysis

Software Excel 2007 (Microsoft, USA) was used to arrange the data set. Software Statistica 10 (StatSoft, USA) was used to perform statistical analysis and chart construction. Signal intensity of western blotting was determined using ImageJ 1.45 software (NIH, USA) as an area under the curve. Viability was determined by quadratic regression of MTT (''MTT viability'') and by fitting a real-time impedance chart at $t = 72$ h, data transposition and regression from the linear part of the curve. *t*-tests were used to reveal significant differences between groups. Simple linear correlations were performed to reveal the relationship between variables. Unless noted otherwise, a level of statistical significance was designated to $p = 0.05$. Scatterplots were fitted with the negative exponentially-weighted fitting algorithm.

Results

Real-time monitoring of cell adhesion and proliferation using the xCELLigence system

The question addressed in this study was whether zinc(II) ions would affect the prostatic cells proliferation and morphology. Zinc(II) metabolism in prostate (cancer) cells has been not entirely clear to date.[10] Primarily, the optimal cell concentration for real-time proliferation and viability assays was determined. Cells in count 5000, 10 000, 15 000, 20 000, 30 000, and 40 000 per well were seeded in E-plate 16 and the measurement was carried out (data not shown). Optimal response was found for the well containing 10 000 cells. For wells with lower cell count, a lower relative impedance signal level was yielded (represented as ''cell index'' in manufacturer's software) and it was associated with higher standard deviation (coefficient of variation: 3.1% and 0.8% in 5000 cells and 10 000 cells, respectively). In contrast, for wells with higher cell count overgrowing of cells on one another was observed when the E-plate was viewed under a microscope. Thus high cell density had inhibitory effects resulting in end of linear increase of relative impedance depending on the cell count (data not shown). Therefore, 10 000 cells per well were used to examine the effect of zinc(II) ions on prostatic cell lines.

Consequently, IC_{50} of zinc(II) on cell lines obtained by MTT cytotoxicity assay were determined. IC_{50} values of zinc(II) treatments were 194.3 μM for non-tumour cells PNT1A and 93.9 μM for PC3 tumour cells (Fig. 3A, Table 1). However, during the first measurements with xCELLigence proliferation and viability assay it was observed that chosen zinc(II) concentrations around and above MTT assay determined IC_{50} values exhibit more cytotoxic effects than was expected (compare Fig. 3A and B). Thus, for the proliferation and viability assay lower zinc(II) ions treatment concentrations were optimized as follows: 0 (control), 25 μM, 50 μM, 75 μM and 100 μM for both cell lines. Both cell lines reach a stationary phase of growth in 160 h. However, apparent difference in relative impedance values

Table 1 Comparison of viability determination, protein content and cell size in cell lines. xCelligence relative impedance, MTT absorbance, cell concentrations, protein content and cell size are displayed as a relative ratio of not treated/treated samples for more obvious comparison. IC_{50} is calculated from these methods. Apparent differences in MTT-determined and xCELLigence-determined IC_{50} are due to different cell size and cell count in PC-3 and PNT1A

		xCelligence		MTT		Cell count		Protein	Cell size
Cell line	Zinc(II) in medium/ μM	Relative impedance (%)	IC_{50}/ μM	Relative viability MTT (%)	IC_{50}/ μM	Relative cell count (%)	IC_{50}/ μM	Relative concentration (%)	Relative cell (%)
PC-3	0	100.0	55.5	100.0	93.9	100.0	60.7	100.0	100.0
	25	89.5		101.4		84.6		72.6	112.2
	50	33.1		101.4		102.0		94.4	88.2
	75	9.7		92.0		2.0		71.8	81.1
	100	3.0		7.8		0.4		14.5	74.1
PNT1A	0	100.0	150.8	100.0	194.3	100.0	131.3	100.0	100.0
	25	98.1		99.3		112.5		102.3	105.3
	50	99.9		98.9		139.2		106.4	111.5
	75	97.9		95.9		140.5		106.4	92.6
	100	87.7		97.0		133.6		98.4	91.6

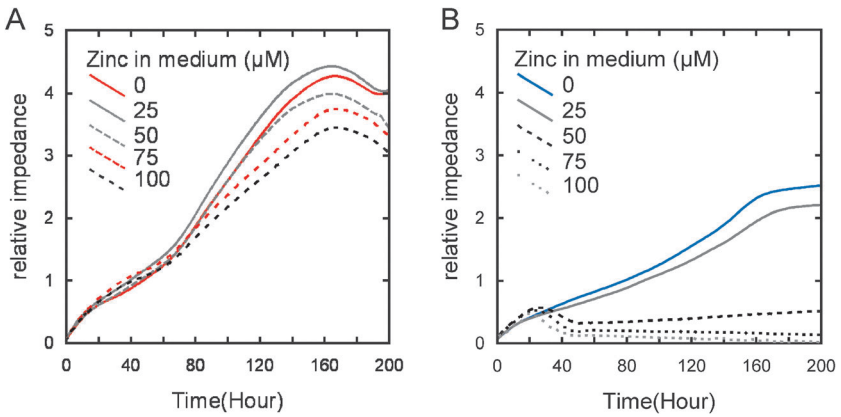

Fig. 2 Real-time monitoring of cell adhesion and proliferation using the xCELLigence system. PNT1A (A) and PC-3 (B) cells were seeded at a density of 10 000 cells per well in E-Plates 16. After 24 hours, zinc(II) sulphate was added and the cell index was monitored. The measurements were done in duplicates.

between cell lines was observed. Tumour cell line PC-3 reached 1.7-fold lower relative impedance in stationary phase of growth as compared to non-tumour cell line PNT1A (compare Fig. 2A and B at 0 μM zinc(II) concentration).

After adding zinc(II) ions (24 h after initiation of the experiment, see Fig. 2A and B), a rapid decrease in relative impedance in less than 2 h after the treatment was observed; it stabilized after 10 h, notably at high zinc(II) concentrations. After the stabilization, a less steep decrease of relative impedance in a concentration-dependent manner was observed. Concentrations of 150 μM in the case of PNT1A and 50 μM and more in the case of PC-3 induced a 2.6-fold and >24.8-fold decrease of relative impedance in PNT1A and PC-3 cell lines, respectively, compared to non-treated samples. On the other hand, zinc(II) concentration of 25 μM induced a 5% increase of the relative impedance value in PNT1A cells. In contrast, no such elevation of cell concentration after zinc(II) treatment is evident in PC-3 cells.

The IC_{50} values of zinc(II) ions using the xCELLigence system were also determined for the same period of time as MTT assay (72 h from the beginning of the experiment). These IC_{50} values were 150.8 μM zinc for PNT1A cells and 55.5 μM zinc for PC-3 cells. Thus, it may be concluded that zinc(II) is toxic to a tumour cell line in 2.7-fold lower concentration (see Table 1). However, IC_{50} values obtained from the xCELLigence system are 1.3-fold and 1.7-fold lower in PNT1A and PC-3 cell line, respectively, than IC_{50} values determined by MTT cytotoxicity assay. Due to this discrepancy MTT and xCELLigence system assays combined with other methods were further compared. It was shown that the relative impedance is influenced mostly by cell count, its adherence and morphology.[11] Hence the area of cells and the total viable cell count were determined in order to assess how these variables affect relative impedance. In terms of average cell area, it was found that PC-3 cells are 2-fold larger compared to PNT1A cells (135.1 ± 14.6 μm^2 and 67.7 ± 5.4 μm^2) (Fig. 3D). When treated with zinc(II), PNT1A cells do not show differences in cell size, whereas PC-3 cells area decrease with increasing zinc(II) treatment concentration (Fig. 3D). Then the cell content was determined and it was found that PC-3 cell lines achieved 1.6-fold smaller cell count at the same time interval (48 h) as compared to PNT1A (686.4 ± 46.1 cells per μl and 1083.8 ± 33.7 cells per μl in PC-3 and PNT1A cell line, respectively) (Fig. 3C). Significant statistical correlation ($r > 0.92$; $p < 0.03$) between results from the xCELLigence system and viable cell count during zinc(II) treatments was found. On the other hand, no significant correlation between xCELLigence system monitoring and MTT assay ($r > 0.80$; $p < 0.10$) was observed.

Cytology and gene expression

Primarily, this study focused on general cytology of both PC-3 and PNT1A cell lines. For these purposes, acridine orange (AO) was used. Acridine orange can serve as a marker of the lysosomal proton pump, an important marker of lysosomal function.[12] Treatment of PC-3 and PNT1A cell cultures with zinc(II) ions led to significant changes in cell morphology and especially in the formation of a monolayer. In control cells and cells treated at zinc(II) concentrations of 50 and 75 μM, lysosomes are well evident and their visualisation is connected with functioning of the lysosomal proton pump. Under higher zinc(II) concentrations (100 μM), lysosomes are not visible, but cytoplasm diffusely emits in the red area.

On the other hand, AO can be used for monitoring the RNA biosynthesis.[13] The incorporation of AO into nucleic acids depends on their structure. Double-helical DNA forms enable emission of AO at an emission maximum of 530 nm (green fluorescence), simpler non-helical RNA organization leads to the shift of AO emission at 660 nm (not shown). There are distinctive differences between cell lines in terms of RNA synthesis. RNA localisation is possible in nucleoli and cytoplasm. Whereas increased RNA synthesis in "healthy", non-tumour cell line PNT1A is evident only at higher zinc(II) ion concentrations (100 μM), increased RNA synthesis in tumour cell line PC-3 is apparent in all variants – in control (untreated cells) as well as cells treated at all zinc(II) ion concentrations (not shown). Similarly, the nucleoli, *i.e.* sites of RNA localization, are clearly visible in the control and in all treated cells of tumour cell line PC-3. On the other hand, in "healthy" non-tumour PNT1A cells the nucleoli are visible only in the cells treated with the two highest zinc(II) concentrations. This also corresponds to increased RNA biosynthesis at these two concentrations.

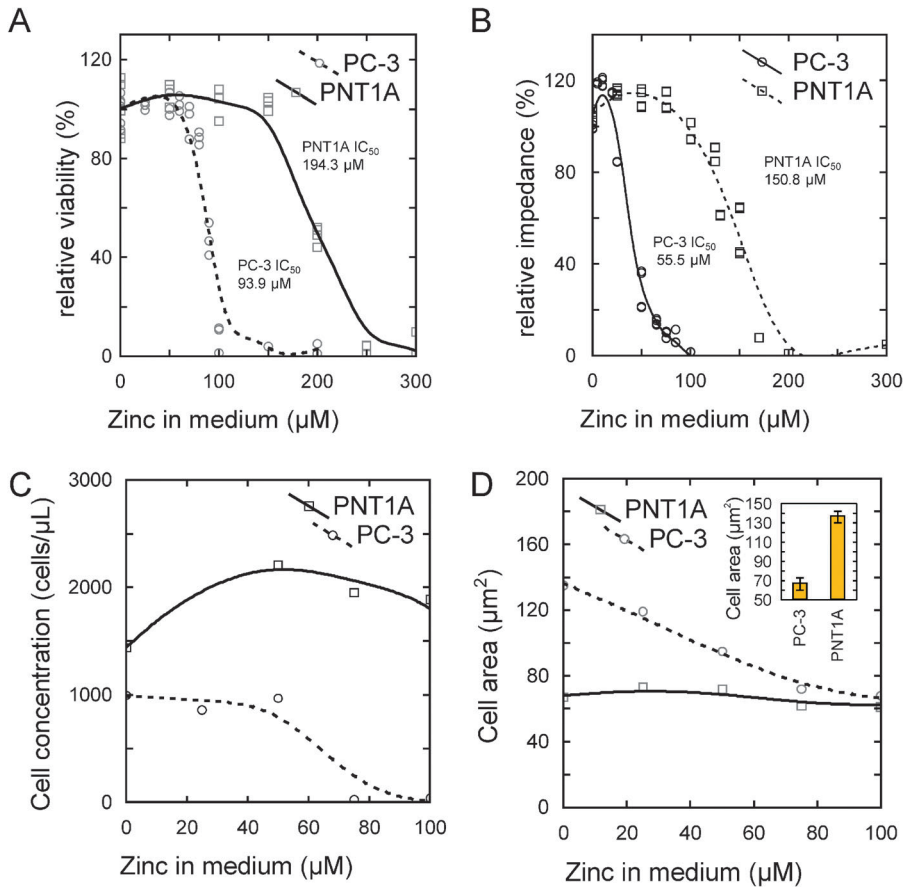

Fig. 3 Comparison of MTT, xCELLigence and cell concentration viability and cell size. (A) MTT-determined response to zinc(II) treatment, (B) xCELLigence determined response to zinc(II) treatment. Significantly higher IC_{50} are reached compared to xCELLigence-determined viability (A *vs.* B). (C) Dependency of cell count on zinc(II) treatment. Cell concentration in relation to zinc(II) treatment is elevated at concentrations of 50–100 µM in PNT1A compared to PC-3 cell lines. (D) Cell size in response to zinc(II) treatment. The PC-3 cell area is reduced during zinc(II) treatment, PNT1A maintains the same cell size. Whereas xCELLigence impedance monitoring is influenced by cell count and cell size, due to (D) is more pronounced decrease of viability in (B) in the PC-3 cell line compared to MTT (A). (D, inset): cell area in cell lines not exposed to zinc treatment (mean ± SD).

Determination of free and bound zinc(II) cellular levels after zinc(II) exposure

To investigate the relationship between zinc(II) metabolism, MT1 and MT2 gene expression and the cell redox state, the levels of intracellular free and protein bound zinc(II) ions were determined. To allow comparison of zinc(II) levels between various samples, the determined zinc(II) content was related to the viable cell count (relative impedance determined by xCELLigence assay (zinc concentration µM/relative impedance)). When the untreated cell lines were compared, significantly higher cellular bound (2.1-fold) and significantly lower free zinc(II) levels (2.3-fold) were found in non-tumour PNT1A cells as compared to PC-3 cells (compare insets in Fig. 4A and B).

After the zinc(II) treatment, a significant enhancement of the bound and free intracellular zinc(II) forms was observed in both cell lines. This increase correlated with zinc(II) concentration in growth medium at $r = 0.91$ ($p = 0.03$) and 0.98 ($p = 0.003$) for free and bound zinc(II) in the PC-3 cell line and at $r = 0.86$ ($p = 0.02$) and 0.98 ($p = 0.001$) for free and bound zinc(II) in the PNT1A cell line, respectively. When 100 µM zinc(II) treatment is compared to non-treated samples, 4.1-fold increase of bound zinc(II) and 3.5-fold increase of free zinc(II) were observed in PNT1A cells. In contrast, a more pronounced increase was detected in bound (5.7-fold) and free (30-fold) zinc(II) fractions in PC-3 cells.

Consequently, the zinc(II) content was determined by the use of fluorescent microscopy. Localisation of free zinc(II) ions with the use of fluorescent probe *N*-(6-methoxy-8-quinolyl)-*p*-toluene sulphonamide, which is specific for these ions, led to detection of differences between free zinc(II) ions localisation in non-tumour PNT1A cells and tumour PC-3 cells. In PC-3 cells, the amount of free zinc(II) ions is connected with treatment (not shown). At the lowest zinc(II) concentration, decrease of emission intensity is well evident. At other zinc(II) concentrations in this cell line intensity of emission increases. At the highest zinc(II) concentration (100 µM), localisation of these ions around nuclei, in nuclei and in the inner part of cytoplasm in the form of spots is well visible. Peripheral parts of cytoplasm demonstrate only weak emission, representing only low free zinc(II) levels in these localizations. In PNT1A cells, intensity of emission of the fluorescence product between the above-mentioned fluorescent probe and free zinc(II) significantly increases with increased supplementation of cultivation medium

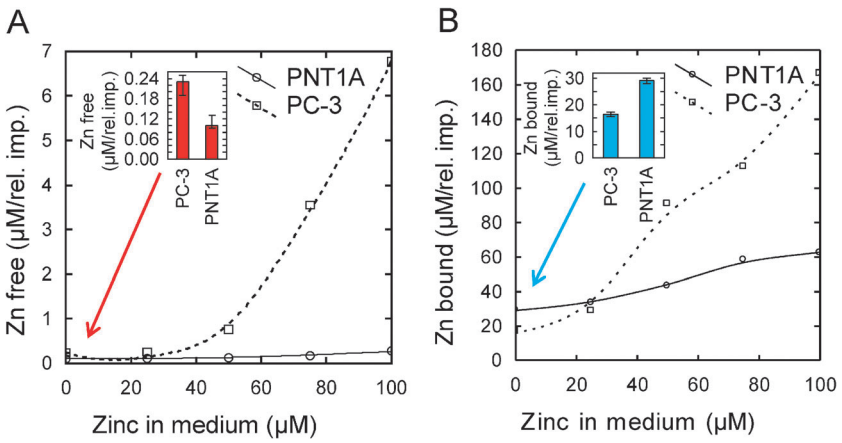

Fig. 4 Intracellular zinc in cell lines. (A) Intracellular free zinc(II) content in human prostate cells human prostatic tumour (PC-3) and normal prostatic (PNT1A) cells treated with 0–100 μM of zinc(II) sulphate. Both cell lines elevate intracellular free(II) zinc. Intracellular free zinc(II) content in untreated samples (A, inset, mean ± SD), significantly higher free zinc in PC-3 cell line. (B) Response to zinc, intracellular bound zinc fraction; bound zinc(II) in untreated samples (B, inset, mean ± SD). Untreated PC-3 cell lines show lower bound zinc, but demonstrate more distinct increase when treated.

by zinc(II) (not shown). Localisation of free zinc(II) is also well visible – at the lowest concentration (25 μM) around nuclei (Golgi, endoplasmic reticulum) and in nuclei. With increasing zinc(II) concentration, increase in the level of free zinc(II) around nuclei is visible. In comparison with tumour cell line PC-3, PNT1A cells did not demonstrate localisation of free zinc(II) in the form of spots.

Effect of zinc(II) on the expression of MT1 and MT2 mRNA and protein levels in prostate cells

Further, this study was focused on two MT isoforms (MT1A and MT2A) at the RNA level and at the level of translated proteins. It is shown in Fig. 5 that zinc(II) treatment has different effects on transcriptional and translational levels of MT1 and MT2 in prostate cells. The zinc(II) effect on the transcription level of MT1 and MT2 was studied by RT-PCR. We found no significant difference ($p > 0.05$) in MT1A and MT2A mRNA levels between cell lines (Fig. 5C). When the level of MT isoforms is compared, significantly ($p < 0.001$) a higher MT2A mRNA level (12-fold) is found in both cell lines. No distinct level change of MT1A mRNA isoform was observed when exposed to zinc(II) treatment (Fig. 5A). In contrast, significant up-regulation of MT2A isoform was observed in PC-3 ($r = 0.99$; $p = 0.001$) and PNT1A ($r = 0.89$; $p = 0.039$) cell lines (Fig. 5B). More distinct elevation in MT2A class mRNA was observed in the PC-3 cell line (80-fold).

Then the MT1 and MT2 at a protein level using western blot assay were determined (Fig. 5F). When treated with zinc(II), the PC-3 cell line showed >4-fold increase in the MT level. In the PNT1A cell line, no such trend was observed. To refine the detection of MT by a sensitive method, the level of endogenous MT1 and MT2 proteins using differential pulse voltammetry Brdicka reaction was determined.[14] To normalise the protein content, values were related to viable cell count (relative impedance determined by xCELLigence assay (MT concentration nM/relative impedance)). Untreated PC3 cells produced 3.6-fold more MT protein as compared to PNT1A cells (Fig. 5E, inset), 15.6 ± 1.1 ng per rel. imp. and 4.2 ± 0.2 ng per rel. imp., respectively. After zinc(II) treatment apparent differences in MT protein in cell lines were observed. Whilst the PNT1A cell line showed mild 4.2-fold increase after zinc(II) treatment (17.7 ± 0.9 ng per rel. imp. MT at 100 μM zinc(II) concentration, positive correlation at $r = 0.94$ and $p = 0.005$), the PC-3 cell line showed more distinct increase in the MT protein level after the treatment. When PC-3 cells were treated with 100 μM zinc(II), 147.2 ± 3.2 ng per rel. imp. MT1 and MT2, *i.e.* tenfold increase was observed. Thus, these results were in good accordance with western blot analysis. Our results show that MT2 RNA and MT protein maintain the same increasing trend in both cell lines (Fig. 5B and E) and thus significant correlation ($r = 0.94$ at $p = 0.017$) was observed. However, although a similar increasing trend was observed in the PNT1A cell line, it was below the level of statistical significance ($r = 0.72$; $p = 0.102$).

Cell redox state

Microscopic detection of proteins with free –SH groups is enabled by the use of the specific probe 5-(bromomethyl)fluorescein, which includes formation of the fluorescent product after reaction with –SH groups of thiols. In the PNT1A non-tumour cells, the amount of proteins with free –SH groups continually decreases with increasing zinc(II) ions supplementation. At the highest concentration, proteins with free –SH groups are visible practically only in newly originated cells, whereas in older cells their amount is only omissible. In this cell line, distribution of thiols takes place especially around nuclei and in nuclei, and is limited in peripheral parts of cells. Compared to PNT1A, contradictory results were obtained for the tumour PC-3 cell line: increasing supplementation of cultivation medium by zinc(II) ions led to increased synthesis of proteins with free thiol group/groups localised in nuclei and especially around nuclei in endoplasmic reticulum and Golgi apparatus (not shown).

Discussion

Real-time monitoring of cell adhesion and proliferation using the xCELLigence system

Standard methods for cell viability or proliferation determination include time-consuming end-point analysis assays of

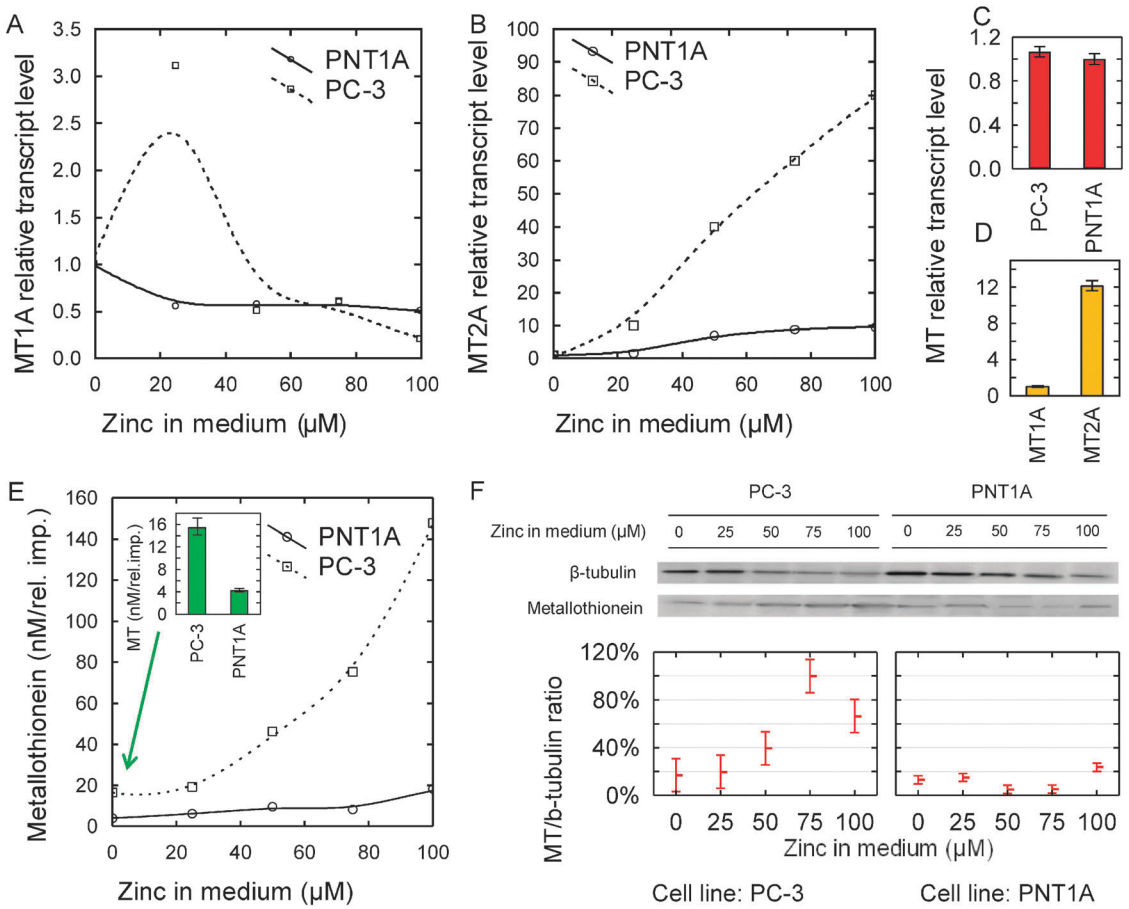

Fig. 5 Determination of MT1A and MT2A expression in PNT1A and PC-3 cells by qRT-PCR and MT1/2 by Western blot analysis and electrochemistry. Metallothionein MT1A (A) and MT2A (B) isoform mRNA levels in cell lines exposed to zinc(II) treatment, (C) total relative MT mRNA levels in untreated samples, (D) relative levels of MT1A and MT2A in untreated samples, (E) metallothionein protein levels exposed to zinc and in untreated samples (inset, displayed as mean ± SD), (F) Western-blot MT detection. Level of MT displayed as a ratio to β-tubulin from the same samples.

whole cell populations (MTT or XTT assays) and advanced techniques of analysis of individual cells (flow cytometry or digital microscopic techniques and image analysis). However, these techniques are not capable of registering very small and rapid changes in cellular morphology.[15] Most of the studied compounds used for various cell treatments in experiments have different effects not only on cell viability but also on cell proliferation, cell adhesion and spreading. These effects are highly dynamic and may also show differences in various cell types. This is evident from different values of IC_{50} obtained by MTT and xCELLigence assays (1.3- and 1.7-fold higher in PNT1A and in PC-3 when using MTT assay). More pronounced difference in PC-3 may be explained by decrease of its cell size in relation to zinc(II) treatment compared to PNT1A, where no size change is observed (Fig. 3D). In the case of the PNT1A cell line, under 25 μM zinc(II) treatment the relative impedance is approx. 5% increased as it is evident from proliferation assay. It is evident from Fig. 3C and D that average cell area of PNT1A cells is relatively stable but number of cells increased. Such 5% increase of impedance therefore represents a higher cell proliferation rate in PNT1A cells (higher cell concentration *vs.* stable cell size).

It may be concluded from the present findings that the xCELLigence assay reflects more the cell concentration than its MTT-based metabolic activity. This conclusion is supported by the fact that xCelligence correlates significantly with the cell count and not with MTT results. We believe that determination of cell viability/cytotoxicity of compounds used in experiments by conventional methods like MTT or XTT is not sufficient. It brings out only end-point analysis of the state of whole cell populations which cannot capture important effects of treatments on proliferation dynamics. Here we demonstrated that the xCELLigence system represents an ideal tool for identification of the onset and the rate of cytotoxicity and for determination of the optimal time point for further molecular and biochemical analyses of cellular events. Moreover, the real-time data stream of the xCELLigence system provides a continuous, label-free measure of cell culture quality.

Zinc, metallothionein and redox state

It has been demonstrated in numerous studies that healthy prostate tissue accumulates a distinctly higher zinc(II) content compared to other cells and this accumulation is altered in prostate cancer tissue.[1a,c] These findings are summarised in the work by Costello and Franklin.[10] They reported that the mean decrease of tissue zinc(II) in cancer tissue compared to healthy tissue is −62% ± 5%. In healthy tissue, a high zinc(II) level is

crucial for the proper functioning and proliferation of the gland.[16] The high level induces apoptosis and inhibits cell growth, whereas the lower level may create an environment more suitable for tumour progression.[17] Zinc transporters, notably ZIP1, play a key role in zinc(II) accumulation and some of them (to date described in ZIP1–3) are down-regulated in prostate cancer. They can therefore be considered as tumour suppressors.[18]

To date, there has been only limited evidence studying zinc(II) levels and effects of zinc(II) treatment on prostate cancer cell line PC-3 and no evidence studying zinc(II) levels in healthy prostate cell line PNT1A. We have demonstrated approx. −48% decrease of (bound) zinc(II) content in prostate cancer cell line PC-3 in comparison to non-tumour PNT1A. According to the study by Feng *et al*., the intracellular zinc(II) level in the PC-3 cell line is decreased −53% compared to non-tumour HPR-1 cell lines.[17a] Although different non-tumorous cell lines were used in this study, the authors obtained similar results. Our results are also in good agreement with results obtained from *in vivo* biopsies in 16 studies summarised by Costello and Franklin[10] (see the previous paragraph) suggesting that PC-3 and PNT1A cell lines may represent zinc(II) buffering conditions *in vivo*.

When exposed to zinc treatment, we observed elevation of both bound and free zinc(II) fractions in both cell lines suggesting that even tumour PC-3 cell line has retained zinc-transport mechanisms. Interestingly, tumour cell line PC-3 shows much more distinct increase in free and bound zinc fractions compared to PNT1A. When treated with 100 μM zinc(II), elevation of intracellular bound zinc levels up to the two-fold concentrations of non-tumour cell line PNT1A was observed in PC-3 (compare Fig. 4A and B). This trend was not only occurring in the bound zinc(II) fraction, but also free zinc(II) demonstrated a similar trend. However, under these conditions (100 μM zinc(II) treatment) the PC-3 cell line retains only approx. 3% viability compared to the untreated sample (Fig. 3A, Table 1). In contrast, the PNT1A cell line still retains high viability when treated with 100 μM zinc(II) (88%). According to these results, it is possible to argue that the increased rate of apoptosis/necrosis is associated rather with an increased relative ratio of intracellular zinc(II) (ratio of zinc after treatment/zinc before treatment) than only with the absolute amount of zinc(II) treatment concentration in the medium. This may be evidenced from the fact that there is an elevation of bound zinc (2.7-fold and 5-fold for PNT1A and PC-3, respectively) after exposure to concentrations equal to IC_{50} of these lines (150 μM and 56 μM for PNT1A and PC3, respectively). This is in agreement with the study by Feng *et al*., which has previously demonstrated a similar difference between tumour and non-tumour cell lines – exposure to zinc induced apoptosis in PC-3 and BPH cells, which accumulate high intracellular levels of zinc(II), but not in HPR-1 cells, which do not accumulate high levels of zinc(II).[17a]

For visualization of general cytology and distribution of free zinc(II) and thiols with free –SH groups, a modified method of cell cultivation directly on microscopic slides was used. This technique enables easy manipulation of cells growing in monolayers including staining and washing steps as well as excellent visualization of cell structures without the necessity of usage of confocal microscopy.[19] Microscopic observations in our study fully confirmed precise analytical data and enabled localisation (not shown) of structures and compounds of interest directly in studied cells. Regarding the results of electrochemistry and microscopy, similar increasing trends in free zinc(II) levels were observed in both cell lines after zinc(II) treatment. Also more intense fluorescence in the PNT1A cell line was observed where higher free zinc(II) content was determined using electrochemistry. In PC-3 cells, decrease of emission is probably caused by their linkage to competent proteins. At other zinc(II) concentrations intensity of emission increases. Generally, distribution of free zinc(II) ions in PC-3 cells is well evident in cytoplasm surrounding nuclei and in nuclei, where zinc(II) ions play a crucial role in activation and/or regulation of transcription due to formation of zinc(II) fingers. In comparison to tumour cell line PC-3, PNT1A cells did not demonstrate localisation of free zinc(II) in the form of spots. These results are partly in agreement with the studies by Feng *et al*.[17a,20] and Wei *et al*.,[21] which demonstrated 4.3-fold elevation of zinc(II) levels in PC-3 after 15 μM (exactly 1 μg ml^{-1}) zinc(II) treatment. Intracellular zinc(II) elevation was determined as 1.5-fold increase (under 25 μM zinc(II) treatment). According to our knowledge, no previous study did show effects of zinc(II) treatment on PNT1A cell lines and therefore our findings cannot be compared to any other results. The above-mentioned work by Feng *et al*. used the HPR-1 cell line as a model of non-tumorous tissue. To date, prostate-specific direct effects of zinc(II) on apoptosis have been well-identified and are discussed in the following reviews.[20,22]

When fluorescent microscopy was utilised in the determination of RNA biosynthesis, notable differences, probably connected with zinc(II) ions treatment, were evident. Whereas increased RNA synthesis in PNT1A is evident under higher zinc(II) ion concentrations, increased RNA synthesis in tumour cell line PC-3 is well evident at all concentrations (not shown). In comparison to nucleoli of both cell lines, sites of RNA localization are well evident in control and all treated cells of tumour cell line PC-3. In non-tumour PNT1A cells, nucleoli are visible only at the two highest zinc(II) concentrations, which also correspond to increased RNA biosynthesis at these two concentrations. This fact may be connected with the response of non-tumour PNT1A cells to zinc(II) treatment and resistance of tumour PC-3 cells to zinc(II) ions. This response does not necessarily result in enhanced biosynthesis of thiol compounds (including MTs), but it may also result in synthesis of non-thiol proteins connected with stress (triggered by zinc(II) ions and proteins connected to cellular responses to stress factors, such as proteins of the apoptosis pathway).

Significantly higher MT protein content in the PC-3 cell line was observed compared to the PNT1A cell line in untreated, *e.g*. control samples. Interestingly, no significant difference between cell lines was determined at the mRNA level (compare Fig. 5C and the inset in Fig. 5E). This fact implies that another regulating mechanism in post-translation exists in PC-3 and PNT1A cell lines. Such a regulation mechanism can be based on small RNAs.[23] Inasmuch as MT binds zinc(II) and bound zinc(II) levels are higher in the PC-3 cell line, it is obvious that

MT levels should be higher in this cell line. Binding of "free" zinc(II) ions by MTs diminishes the amount of this metal available to generate free radicals, especially reactive oxygen and nitrogen species.[24] This is in contradiction with the study by Wei *et al*. which also showed a significantly lower MT1/2 protein level in the PC-3 cell line. However, this study used the non-tumour HPR-1 cell line as a control.[21] To date, no study determined the metallothionein content in PNT1A cell lines; comparison with other cell lines gives therefore only approximate results.

When cell lines are treated with zinc(II), increased MT2A mRNA and protein levels in both cell lines and no changes in MT1A mRNA are observed. In our recent studies we found out that MT2A is a major MT isoform in healthy and tumour prostate cell lines PNT1A and 22Rv1.[25] This study show similar results – MT2A is a dominant isoform also in the PC-3 cell line (Fig. 5D). Thus, this explains the fact that a correlation between mRNA and protein is only in MT2A isoform. Interestingly, PC-3 cells exhibit enhanced increase in MT mRNA and protein compared to PNT1A cells. This increase apparently corresponds to the enhanced elevation of endogenous zinc(II) levels after zinc(II) treatment in this cell line, however, it is caused by different expression of zinc(II) transport proteins, the MT-regulating miRNAs, or other mechanisms that have been unknown to date. Using fluorescent microscopy, we observed an increase of –SH fluorescence in the zinc(II)-treated PC-3 cell line and no such distinct changes in fluorescence were observed in the PNT1A cell line, which is in accordance with increasing trend of MT. These findings are in good agreement with works by Wei *et al*., Hasumi *et al*., Lin *et al*., Iguchi *et al*. and Yamasaki *et al*., who in general demonstrated up-regulation of MT expression when exposed to zinc(II) treatment or other stress stimuli.[16b,21,26] Wei *et al*. reported up-regulation of MT gene expression in PC-3 when exposed to zinc(II) treatment. Similarly, Hasumi *et al*. and Iguchi *et al*. found that MT gene expression is zinc-inducible.[16b,26a] Our results are also in agreement with the work by Yamasaki *et al*., who found up-regulated MT-2A expression in the PC-3 cell line under stress conditions such as hypoxia.[27] A study by Lin *et al*. determined expression of various MT1 isoforms after loading 20 μM zinc(II) in the PC-3 cell line.[26b] Interestingly, this study showed only up-regulation of MT-1J and MT-1M gene expression when exposed to zinc(II) and no significant change in MT-1A gene expression when exposed to zinc(II). These data suggest that zinc(II) may act as an isoform-specific MT inductor.

The GSH–GSSG redox pair can be efficiently coupled with MTs and thus can protect cells against oxidative stress (ROS).[4b] Therefore monitoring of the GSH–GSSG ratio with determination of MTs may represent an effective tool for studying zinc(II) effects on cell redox potential. Biological disulphides such as oxidized glutathione (GSSG) oxidize MTs with a concomitant release of zinc, while reduced glutathione (GSH) reduces the oxidized protein to thionein, which then binds the free zinc(II) ions.[28] Conversely, thiol depletion is associated with activating caspase-3 and thus apoptosis.[29] In our experiments, we found some changes in the thiol-containing peptides and proteins and their further study will be needed.

Conclusions

In this study, characteristics of prostatic cell lines PC-3 and PNT1A exposed to zinc(II) treatment determined by novel real-time monitoring system xCELLigence are provided. This system allows description of the cell lines response to metal toxicity more precisely as compared to commonly used end-point assays. Significant differences in IC_{50} determination were found using both methods due to dependence of impedance assay on cell morphology, cell adhesion and cell count and due to changes of those variables when treated with zinc(II). To date, there has been no evidence of the PNT1A cell line in response to zinc(II). Furthermore, elevation of intracellular bound and free zinc(II) in these cell lines after zinc(II) treatment was observed. These results are in good agreement with published studies. Also, the detected level of metallothionein is in agreement with most published results. In our experiments, increased levels of MTs in PC-3 and PNT1A cell lines were found; published results describe in general similar elevation of MTs when exposed to stress conditions such as heavy metals, reactive oxygen species or hypoxia. We also found differences in the GSH–GSSG system between cell lines – zinc(II) treatment caused elevation of reduced thiols in non-tumorous PNT1A cell lines, and no change of thiols in tumorous PC-3 cell lines. This study also demonstrated a comparison of fluorescence microscopy with precise electrochemical techniques and real-time PCR in the determination of intracellular zinc(II) and thiols with a good agreement in results. If employed together, these methods provide accurate information for zinc(II) fluxes, their buffering by thiol compounds and monitoring of the redox state in cell lines or tissues. Thus, an integrated approach with these methods for detection of thiols and heavy metals may be a powerful tool for understanding the role of oxidative stress in carcinogenesis.

Acknowledgements

This work has been supported by the following projects GACR 301/09/P436, NanoBioTECell GA CR P102/11/1068, IGA VFU 43/2011/FaF and CEITEC CZ.1.05/1.1.00/02.0068.

References

1 (*a*) L. Costello and R. Franklin, The intermediary metabolism of the prostate: a key to understanding the pathogenesis and progression of prostate malignancy, *Oncology*, 2000, **59**, 269–282; (*b*) F. K. Habib, Evaluation of androgen metabolism studies in human prostate cancer–correlation with zinc levels, *Prev. Med.*, 1980, **9**, 650–656; (*c*) V. Y. Zaichick, T. V. Sviridova and S. V. Zaichick, Zinc in human prostate gland: Normal, hyperplastic and cancerous, *J. Radioanal. Nucl. Chem.*, 1997, **217**, 157–161.

2 (*a*) D. Beyersmann and H. Haase, Functions of zinc in signaling, proliferation and differentiation of mammalian cells, *Biometals*, 2001, **14**, 331–341; (*b*) D. E. Baranano, C. D. Ferris and S. H. Snyder, Atypical neural messengers, *Trends Neurosci.*, 2001, **24**, 99–106; (*c*) C. Hogstrand, P. Kille, R. I. Nicholson and K. M. Taylor, Zinc transporters and cancer: a potential role for ZIP7 as a hub for tyrosine kinase activation, *Trends Mol. Med.*, 2009, **15**, 101–111.

3 R. A. Colvin, W. R. Holmes, C. P. Fontaine and W. Maret, Cytosolic zinc buffering and muffling: Their role in intracellular zinc homeostasis, *Metallomics*, 2010, **2**, 306–317.

4 (*a*) P. J. Thornalley and M. Vasak, Possible Role for Metallothionein in Protection against Radiation-Induced Oxidative Stress – Kinetics and Mechanism of Its Reaction with Superoxide and

Hydroxyl Radicals, *Biochim. Biophys. Acta*, 1985, **827**, 36–44; (*b*) T. Eckschlager, V. Adam, J. Hrabeta, K. Figova and R. Kizek, Metallothioneins and Cancer, *Curr. Protein Pept. Sci.*, 2009, **10**, 360–375; (*c*) S. Krizkova, P. Blahova, J. Nakielna, I. Fabrik, V. Adam, T. Eckschlager, M. Beklova, Z. Svobodova, V. Horak and R. Kizek, Comparison of Metallothionein Detection by Using Brdicka Reaction and Enzyme-Linked Immunosorbent Assay Employing Chicken Yolk Antibodies, *Electroanalysis*, 2009, **21**, 2575–2583.

5 S. Krizkova, I. Fabrik, V. Adam, P. Hrabeta, T. Eckschlager and R. Kizek, Metallothionein—a promising tool for cancer diagnostics, *Bratislava Med. J.*, 2009, **110**, 93–97.

6 (*a*) V. Adam, I. Fabrik, T. Eckschlager, M. Stiborova, L. Trnkova and R. Kizek, Vertebrate metallothioneins as target molecules for analytical techniques, *TrAC, Trends Anal. Chem.*, 2010, **29**, 409–418; (*b*) V. Adam, J. Petrlova, J. Wang, T. Eckschlager, L. Trnkova and R. Kizek, Zeptomole Electrochemical Detection of Metallothioneins, *PloS One*, 2010, **5**, 569.

7 (*a*) K. Sigler, J. Chaloupka, J. Brozmanova, N. Stadler and M. Hofer, Oxidative stress in microorganisms – I – Microbial *vs.* higher cells – Damage and defenses in relation to cell aging and death, *Folia Microbiol. (Dordrecht, Neth.)*, 1999, **44**, 587–624; (*b*) P. Storz, Reactive oxygen species in tumor progression, *Front. Biosci.*, 2005, **10**, 1881–1896.

8 K. Kubo, Y. Sakita and T. Minami, Effect of heat treatment on metallothionein isoforms using capillary zone electrophoresis, *Analysis*, 2000, **28**, 366–369.

9 (*a*) D. Potesil, J. Petrlova, V. Adam, J. Vacek, B. Klejdus, J. Zehnalek, L. Trnkova, L. Havel and R. Kizek, Simultaneous femtomole determination of cysteine, reduced and oxidized glutathione, and phytochelatin in maize (*Zea mays L.*) kernels using high-performance liquid chromatography with electrochemical detection, *J. Chromatogr., A*, 2005, **1084**, 134–144; (*b*) J. Petrlova, R. Mikelova, K. Stejskal, A. Kleckerova, O. Zitka, J. Petrek, L. Havel, J. Zehnalek, V. Adam, L. Trnkova and R. Kizek, Simultaneous determination of eight biologically active thiol compounds using gradient elution-Liquid Chromatography with Coul-Array detection, *J. Sep. Sci.*, 2006, **29**, 1166–1173.

10 L. C. Costello and R. B. Franklin, Zinc is decreased in prostate cancer: an established relationship of prostate cancer!, *J. Biol. Inorg. Chem.*, 2011, **16**, 3–8.

11 R. J. Keogh, New technology for investigating trophoblast function, *Placenta*, 2010, **31**, 347–350.

12 K. Kusuzaki, H. Murata, H. Takeshita, S. Hashiguchi, T. Nozaki, K. Emoto, T. Ashihara and Y. Hirasawa, Intracellular binding sites of acridine orange in living osteosarcoma cells, *Anticancer Res.*, 2000, **20**, 971–975.

13 K. Lange, R. Herken, K. Keller and H. Herken, Distribution of Acridine Orange-Stained RNA in Neuroblastoma-Cells during Differentiation, *Naunyn-Schmiedeberg's Arch. Pharmacol.*, 1977, **298**, 259–262.

14 I. Fabrik, S. Krizkova, D. Huska, V. Adam, J. Hubalek, L. Trnkova, T. Eckschlager, J. Kukacka, R. Prusa and R. Kizek, Employment of electrochemical techniques for metallothionein determination in tumor cell lines and patients with a tumor disease, *Electroanalysis*, 2008, **20**, 1521–1532.

15 (*a*) E. Urcan, U. Haertel, M. Styllou, R. Hickel, H. Scherthan and F. X. Reichl, Real-time xCELLigence impedance analysis of the cytotoxicity of dental composite components on human gingival fibroblasts, *Dent. Mater.*, 2010, **26**, 51–58; (*b*) J. J. Quereda, L. Martinez-Alarcon, L. Mendoca, M. J. Majado, J. M. Herrero-Medrano, F. J. Pallares, A. Rios, P. Ramirez, A. Munoz and G. Ramis, Validation of xCELLigence Real-Time Cell Analyzer to Assess Compatibility in Xenotransplantation With Pig-to-Baboon Model, *Transplant. Proc.*, 2010, **42**, 3239–3243; (*c*) L. Vistejnova, J. Dvorakova, M. Hasova, T. Muthny, V. Velebny, K. Soucek and L. Kubala, The comparison of impedance-based method of cell proliferation monitoring with commonly used metabolic-based techniques, *Neuroendocrinol. Lett.*, 2009, **30**, 121–127.

16 (*a*) S. Y. Hess, B. Lonnerdal, C. Hotz, J. A. Rivera and K. H. Brown, Recent advances in knowledge of zinc nutrition and human health, *Food Nutr. Bull. Suppl.*, 2009, **30**, S5–S11; (*b*) M. Hasumi, K. Suzuki, H. Matsui, H. Koike, K. Ito and H. Yamanaka, Regulation of metallothionein and zinc transporter expression in human prostate cancer cells and tissues, *Cancer Lett.*, 2003, **200**, 187–195; (*c*) Z. M. Bataineh, I. H. B. Hani and J. R. Al-Alami, Zinc in normal and pathological human prostate gland, *Saudi Med. J.*, 2002, **23**, 218–220.

17 (*a*) P. Feng, T. L. Li, Z. X. Guan, R. B. Franklin and L. C. Costello, Direct effect of zinc on mitochondrial apoptogenesis in prostate cells, *Prostate*, 2002, **52**, 311–318; (*b*) R. G. Uzzo, P. Leavis, W. Hatch, V. L. Gabai, N. Dulin, N. Zvartau and V. M. Kolenko, Zinc inhibits nuclear factor-kappa B activation and sensitizes prostate cancer cells to cytotoxic agents, *Clin. Cancer Res.*, 2002, **8**, 3579–3583.

18 (*a*) R. B. Franklin, P. Feng, B. Milon, M. M. Desouki, K. K. Singh, A. Kajdacsy-Balla, O. Bagasra and L. C. Costello, hZIP1 zinc uptake transporter down regulation and zinc depletion in prostate cancer, *Mol. Cancer*, 2005, **4**, 1–13; (*b*) T. Kambe, Y. Yamaguchi-Iwai, R. Sasaki and M. Nagao, Overview of mammalian zinc transporters, *Cell. Mol. Life Sci.*, 2004, **61**, 49–68; (*c*) R. B. Franklin, J. Ma, J. Zou, Z. Guan, B. I. Kukoyi, P. Feng and L. C. Costello, Human ZIP1 is a major zinc uptake transporter for the accumulation of zinc in prostate cells, *J. Inorg. Biochem.*, 2003, **96**, 435–442; (*d*) B. C. Milon, A. Agyapong, R. Bautista, L. C. Costello and R. B. Franklin, Ras Responsive Element Binding Protein-1 (RREB-1) Down-regulates hZIP1 Expression in Prostate Cancer Cells, *Prostate*, 2010, **70**, 288–296.

19 J. Vitecek, J. Petrlova, V. Adam, L. Havel, K. J. Kramer, P. Babula and R. Kizek, A fluorimetric sensor for detection of one living cell, *Sensors*, 2007, **7**, 222–238.

20 P. Feng, T. L. Li, Z. X. Guan, R. B. Franklin and L. C. Costello, The involvement of bax in zinc-induced mitochondrial apoptogenesis in malignant prostate cells, *Mol. Cancer*, 2008, **7**, 1–6.

21 H. Wei, M. M. Desouki, S. Lin, D. Xiao, R. B. Franklin and P. Feng, Differential expression of metallothioneins (MTs) 1, 2, and 3 in response to zinc treatment in human prostate normal and malignant cells and tissues, *Mol. Cancer*, 2008, **7**, 1–11Artn 7.

22 (*a*) J. Gumulec, M. Masarik, S. Krizkova, V. Adam, J. Hubalek, J. Hrabeta, T. Eckschlager, M. Stiborova and R. Kizek, Insight to physiology and pathology of zinc(II) ions and their actions in breast and prostate carcinoma, *Curr. Med. Chem.*, 2011, **18**, 5041–5051; (*b*) J. Y. Liang, Y. Y. Liu, J. Zou, R. B. Franklin, L. C. Costello and P. Feng, Inhibitory effect of zinc on human prostatic carcinoma cell growth, *Prostate*, 1999, **40**, 200–207.

23 (*a*) N. Rabiau, H. K. Trraf, M. Adjakly, R. Bosviel, L. Guy, L. Fontana, Y. J. Bignon and D. J. Bernard-Gallon, miRNAs Differentially Expressed in Prostate Cancer Cell Lines after Soy Treatment, *In Vivo*, 2011, **25**, 917–921; (*b*) P. Ostling, S. K. Leivonen, A. Aakula, P. Kohonen, R. Makela, Z. Hagman, A. Edsjo, S. Kangaspeska, H. Edgren, D. Nicorici, A. Bjartell, Y. Ceder, M. Perala and O. Kallioniemi, Systematic Analysis of MicroRNAs Targeting the Androgen Receptor in Prostate Cancer Cells, *Cancer Res.*, 2011, **71**, 1956–1967.

24 (*a*) S. G. Bell and B. L. Vallee, The Metallothionein/Thionein System: An Oxidoreductive Metabolic Zinc Link, *Chembiochem*, 2009, **10**, 55–62; (*b*) S. K. Baird, T. Kurz and U. T. Brunk, Metallothionein protects against oxidative stress-induced lysosomal destabilization, *Biochem. J.*, 2006, **394**, 275–283; (*c*) J. C. Amiard, C. Amiard-Triquet, S. Barka, J. Pellerin and P. S. Rainbow, Metallothioneins in aquatic invertebrates: Their role in metal detoxification and their use as biomarkers, *Aquat. Toxicol.*, 2006, **76**, 160–202; (*d*) M. Ebadi, M. P. Leuschen, H. ElRefaey, F. M. Hamada and P. Rojas, The antioxidant properties of zinc and metallothionein, *Neurochem. Int.*, 1996, **29**, 159–166.

25 J. Gumulec, M. Masarik, S. Krizkova, M. Hlavna, P. Babula, R. Hrabec, A. Rovny, M. Masarikova, J. Sochor, V. Adam, T. Eckschlager and R. Kizek, Evaluation of alpha-methylacyl-CoA racemase, metallothionein and prostate specific antigen as prostate cancer prognostic markers, *Neoplasma*, 2012, **59**, 191–200.

26 (*a*) K. Iguchi, M. Hamatake, R. Ishida, Y. Usami, T. Adachi, H. Yamamoto, K. Koshida, T. Uchibayashi and K. Hirano, Induction of necrosis by zinc in prostate carcinoma cells and identification of proteins increased in association with this induction, *Eur. J. Biochem.*, 1998, **253**, 766–770; (*b*) S. F. Lin, H. Wei, D. Maeder, R. B. Franklin and P. Feng, Profiling of zinc-altered

gene expression in human prostate normal *vs*. cancer cells: a time course study, *J. Nutr. Biochem*., 2009, **20**, 1000–1012.
27 S. Yamasaki, K. Sakata-Sogawa, A. Hasegawa, T. Suzuki, K. Kabu, E. Sato, T. Kurosaki, S. Yamashita, M. Tokunaga and K. Nishida, Zinc is a novel intracellular second messenger, *J. Cell Biol*., 2007, **177**, 637.
28 D. Huska, O. Zitka, V. Adam, M. Beklova, S. Krizkova, L. Zeman, A. Horna, L. Havel, J. Zehnalek and R. Kizek, A sensor for investigating the interaction between biologically important heavy metals and glutathione, *Czech J. Anim. Sci*., 2007, **52**, 37–43.
29 R. N. T. Coffey, R. W. G. Watson, N. J. Hegarty, A. O'Neill, N. Gibbons, H. R. Brady and J. M. Fitzpatrick, Thiol-mediated apoptosis in prostate carcinoma cells, *Cancer (N. Y.)*, 2000, **88**, 2092–2104.
30 R. B. Franklin and L. C. Costello, The Important Role of the Apoptotic Effects of Zinc in the Development of Cancers, *J. Cell. Biochem*., 2009, **106**, 750–757.

